X–ray Observations of TeV Blazars and Multi-Frequency Analysis

Tadayuki Takahashi, [a] Greg Madejski, [b] and Hidetoshi Kubo [c]

[a] *Institute of Space and Astronautical Science, Sagamihara, Kanagawa 229-8510, Japan*

[b] *Lab for High Energy Astrophysics, Code 662, NASA/GSFC, MD 20771, USA*

[c] *Department of Physics, Tokyo Institute of Technology, Meguro-ku, Tokyo 152-8551, Japan*

Abstract

The non-thermal spectra of blazars, observed from radio to GeV/TeV γ–rays, reveal two pronounced components, both produced by radiation by energetic particles. One peaks in the IR - to soft X–ray band, radiating via the synchrotron process; the other, peaking in the high-energy γ–rays, is produced by the Compton process. These spectra – and, in particular, the *ASCA* data – suggest that the origin of the seed photons for Comptonization is diverse. In the High-energy peaked BL Lac objects (HBLs), the dominant seed photons for Comptonization appear to be the synchrotron photons internal to the jet (SSC process). In the quasar-hosted blazars (QHBs), on the other hand, the X–ray band emission is still dominated by the SSC process, while the MeV to GeV range is produced by Comptonization of external photons such as the emission line light. In the context of this three-component model, we derive the magnetic field of 0.1 - 1 Gauss for all classes of blazars. Lorentz factors γ_{peak} of electrons radiating at each peak of the $\nu F(\nu)$ spectra are estimated to be $\sim 10^5$ for HBLs; this is much higher than $\sim 10^3$ for QHBs. This difference is consistent with the fact that the four sources that are known to emit TeV γ–rays (TeV blazars) are all classified as HBLs. Among the TeV blazars, Mkn 421 is one of the brightest and most variable emitters from ultraviolet (eV) to hard γ–ray (TeV) energies, and its correlated inter-band variability suggests that both keV and TeV spectral regimes are produced by the same, most energetic end of the electron population radiating via the synchrotron process in the keV, and the SSC process in TeV band. The multi-frequency observations including TeV energy band provide the best opportunity to understand high-energy emission from blazar jets. In this paper, we discuss results of multi-frequency analysis and review the results of intensive campaigns for Mkn 421 from 1994 to 1998.

Key words: galaxies: active,galaxies: jet, BL Lacertae objects: general, BL Lacertae objects: individual (Markarian 421), quasars: general, gamma-rays: theory

1 Introduction

The launch of the Compton Gamma-Ray Observatory and the major improvements to ground-based Cherenkov telescopes marked the 1990s as the pivotal years in the field of astrophysics at the very highest energies. In particular, the detection of GeV γ–rays from over 50 blazars by the EGRET telescope on CGRO (cf. Mukherjee et al. 1997) established them as a class of extreme "particle accelerators" – on two accounts: they produce the most energetic photons of any known extragalactic cosmic sources, but, assuming isotropic emission, they are also the most luminous. It is generally thought that the non-thermal emission from blazars, observed in virtually every band from radio to GeV/TeV γ–rays, is produced by very energetic particles via both synchrotron and Compton processes. Most of these objects are variable, showing flares with the greatest amplitude at the highest energies of each component, on time scales as short as a day. This underlines the importance of the high-energy emission for any modeling. Via the γ–ray opacity arguments (see, e.g., Mattox et al. 1993), this suggests that the γ–ray emission is produced in a very compact region, moving at relativistic speeds at a small angle towards the observer, most likely in a form of a jet.

Multi-frequency studies of blazars reveal that the overall spectra have at least two pronounced components: the low energy peak (LE) and the high energy peak (HE) (see, e.g., von Montigny et al. 1995). For the blazars showing quasar-like emission lines (QHBs), and for BL Lac objects discovered via radio-selection techniques (the Low-Energy Peaked BL Lac objects, or LBLs), the LE component peaks in the infrared, while in the BL Lacs found using X–rays (the High-Energy Peaked BL Lac objects, or HBLs), it peaks in the ultraviolet or even in soft X–rays (see, e.g., Sambruna, Maraschi, & Urry 1996). The HE component, on the other hand, peaks in the γ–ray band, in the MeV - to - GeV range, and in the case of a few HBLs, it extends to the TeV range.

The local power-law shape, the smooth connection of the entire radio - to - UV (and, for the HBLs, soft X–ray) continuum, as well as the relatively high level of polarization observed from radio to the UV, implies that the emission from the LE component is most likely produced via the synchrotron process by relativistic particles radiating in magnetic field. The HE component is then believed to be produced via Comptonization by the same particles that radiate the LE component. The source of the "seed" photons can be the synchrotron radiation internal to the jet – as in the Synchrotron-Self-Compton (SSC) models (Rees 1967; Blandford & Konigl 1979; Konigl 1981; Ghisellini & Maraschi 1989, Inoue & Takahara 1996). Alternatively, these photons can be external to the jet, as in the External Radiation Compton (ERC) models: either the UV accretion disk photons (Dermer, Schlickeiser, & Mastichiadis 1992), or these UV photons reprocessed by the emission line clouds and/or inter-cloud medium (Sikora, Begelman, & Rees 1994; Blandford & Levinson 1995), or else, IR radiation ambient to the host galaxy (Sikora et al. 1994). The X–ray regime is important, as it is where the emission due to both processes overlap: in the context of the above scenario, in HBLs, X–rays form the high energy tail of the synchrotron emission, while for QHBs, they form the lowest observable energy end of the Comptonized spectrum.

The discovery of the TeV emission from four nearby BL Lac objects (Mkn 421, Mkn 501, 1ES2344+514, and PKS 2155-304) by ground based Cherenkov telescopes (Punch et al. 1992; Quinn et al. 1996; Catanese et al. 1998; Chadwick et al. 1998) has given us an opportunity to study the radiation processes responsible for production of photons at such extreme energies. The first multi-frequency observation from Mkn 421 from radio to TeV γ–rays, conducted in 1994, revealed that while the keV X–ray and TeV γ–ray fluxes varied nearly simultaneously, the flux in other bands remained relatively steady (Macomb et al. 1995; Takahashi et al. 1996a). Subsequent multi-frequency campaigns for this object also revealed correlated flare activity in X–rays and TeV γ–rays, suggesting that both keV and TeV spectral regimes are produced by the same, most energetic end of an electron population, radiating via the synchrotron process in the keV band, and Compton process in the TeV bands. Given the relative absence of emission lines in the TeV - emitting HBLs, the "seed" photons for Comptonization are most likely internal to the jet, as in the SSC models.

The multi-frequency spectra of HBLs Mkn 501 and PKS 2155-304 are similar to that of Mkn 421: the LE components of these objects peak in the X–ray band. Mkn 501 showed a remarkable flare activity in April 1997. During the multi-frequency campaign, both X–ray and TeV γ–rays increased by more than one order of magnitude from quiescent level (Catanese et al. 1997; Pian et al. 1998; Kataoka et al. 1999), suggesting that the same mechanism takes place as in the case of Mkn 421. However, in Mkn 501, the synchrotron emission in quiescence peaked below 0.1 keV, while during the 1997 flare, it peaked at $\sim$ 100 keV. This is in contrast to Mkn 421, where the position of the LE peak shows relatively little change. For PKS 2155-304, one of the best studied BL Lac objects in other bands, the TeV emission was detected only recently (Chadwick et al. 1998), most likely due to its Southern location, and a relative lack of TeV telescopes in the Southern hemisphere. PKS 2155-304 had shown very different behavior in two subsequent campaigns (Brinkmann et al. 1994; Urry et al. 1997; Ghisellini et al. 1998).

Here, we report the results of *ASCA* observation of blazars in the context of their multi-frequency emission. Based on the analysis of multi-frequency spectra, we discuss characteristics of TeV blazars. We then review results obtained from our extensive campaigns of one of the brightest TeV blazars, Mkn 421.

2 ASCA Observations of Blazars

ASCA observed 18 blazars, of which 10 were also observed contemporaneously with *EGRET* as parts of multi-wavelength campaigns, and these show a clear difference in the spectra and variability between HBLs, LBLs, and QHBs. We constructed the multi-frequency spectral energy distributions for these 18 sources and performed multi-frequency analysis to study fundamental parameters in the emission from blazars (Kubo 1997; Takahashi et al. 1997; Kubo et al. 1998, hereafter KTM98).

Two examples of blazar spectra plotted in $\nu F(\nu)$ representation (giving the emitted power per decade of energy under an assumption of isotropic emission) are shown in Figure 1. One is of Mkn 421 (Macomb et al. 1995; Takahashi et al. 1996a), a fairly typical HBL; its X–ray spectrum is soft (steep) and on the extrapolation of the ultraviolet, suggesting that the synchrotron emission extends into the X–ray range. The other is PKS 0528+134 (KTM98), a strong lined QHB; in contrast to Mkn 421, the X–ray spectrum of PKS 0528+134 is harder than the UV spectrum, implying that the X–rays form the onset of the second, HE component.

The *ASCA* X–ray spectra of HBLs are the softest, with the power law energy index $\alpha \sim 1 - 2$. The X–ray spectra of the QHBs are the hardest ($\alpha \sim 0.6$). For LBLs, the spectra are intermediate; in one case, 0716+714, the spectrum shows hardening with an increasing energy. The differences in the spectra between subclasses were also observed with *ROSAT* in the soft X–ray band (Sambruna et al. 1996; Urry et al. 1997; Sambruna 1997; Padovani, Giommi, & Fiore 1997; Comastri et al. 1997). While for HBLs, the spectral index often varies with intensity on a time scale shorter than a week, for QHBs, it remains almost constant when the flux changes.

3 Multi-frequency Analysis - Magnetic Field and Electron Lorentz Factors

In the very broadest sense, the overall spectra of blazars can be characterized by four parameters: the peak frequency of the synchrotron and Compton components (ν_{sync} and ν_{Comp}), and luminosity of each component (L_{sync} and L_{Comp}, calculated in the observer's frame, and assuming isotropy of emission).

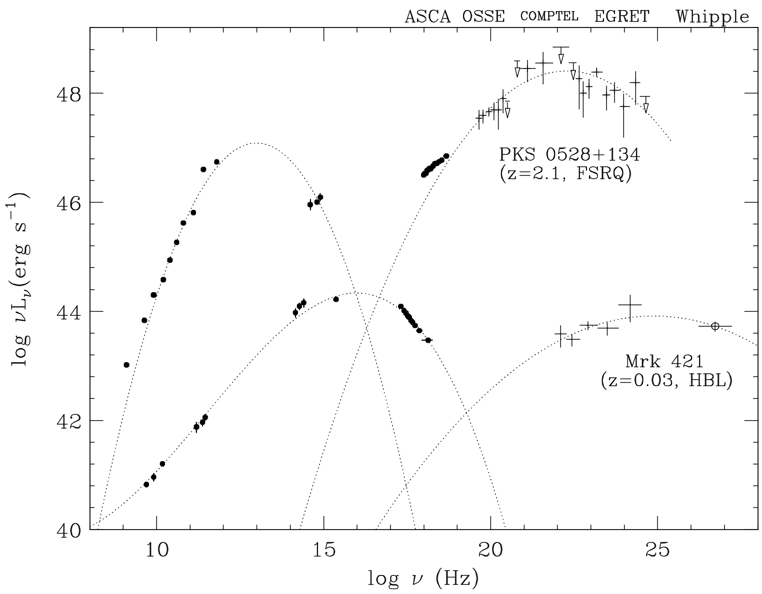

Fig. 1. The multi-frequency spectrum obtained from the simultaneous observations of Mkn 421 and PKS 0528+134. The dotted line shows the results of fit to a third-order polynomial function for low and high energy components.

Fig. 2 shows the distribution of the ratio L_{Comp}/L_{sync} as a function of the peak of the LE component of the blazars considered by KTM98. In QHBs, the ratio is much higher than that obtained from HBLs. In the context of the synchrotron model, ν_{sync} and L_{sync} are determined by the intensity of the magnetic field and the distribution function of electron energies. Similarly, in the context of the Compton model, ν_{Comp} and L_{Comp} are related to the distribution functions of electron and target photon energies. Below, we summarize a formalism useful for the determination of the magnetic field B and electron Lorentz factors γ_{el}, following that presented in Takahashi et al. (1996a) and in KTM98.

When the radiation is due to a single population of relativistic electrons with a broken power law distribution of γ_{el} and a break at γ_{peak}, ν_{sync} (as measured in the observer's frame) is given as:

$$\nu_{sync} = 1.2 \times 10^6 \gamma_{peak}^2 B \frac{\delta}{(1+z)} \quad \text{(Hz)}. \tag{1}$$

Here B is magnetic field in Gauss, measured in the comoving frame, and δ is the "beaming" (Doppler) factor defined as $\delta = \Gamma_j^{-1}(1 - \beta\cos\theta)^{-1}$.

In the case when the photons internal to the jet dominate the radiative energy density (such as in HBLs), $L_{Comp} = L_{SSC}$ and $\nu_{Comp} = \nu_{SSC}$. If the electron energy is still in the Thomson regime, ($\gamma_{el} \times h\nu_{sync} << m_e c^2$), the expected peak of the SSC component is $\nu_{SSC} = 4\gamma_{peak}^2 \nu_{sync}/3$. The ratio of L_{SSC} to L_{sync} is then determined by the intensity of magnetic field, and the distribution

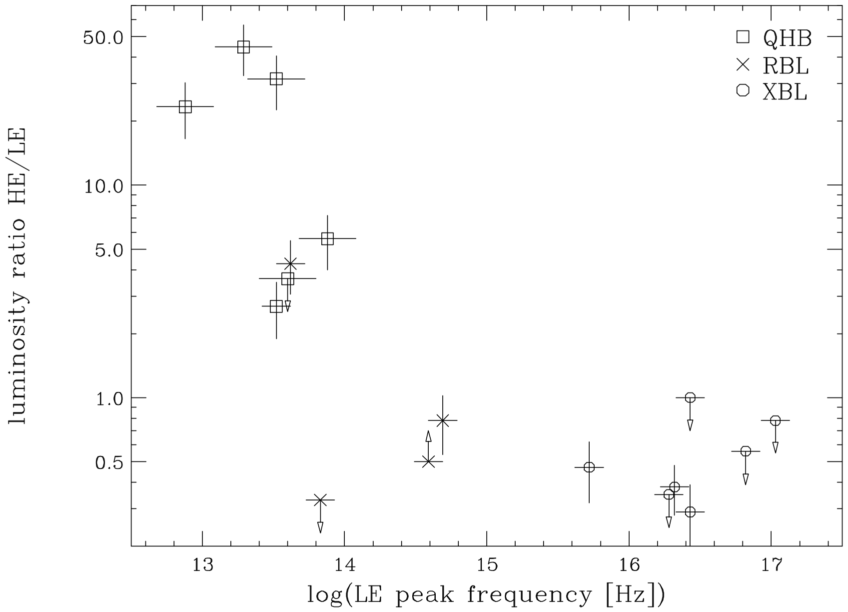

Fig. 2. Distribution of the ratio L_{Comp}/L_{synch} as a function of the peak frequency of the LE component. Arrows indicate the upper or lower limits measured with γ–ray observations.

function of electron energies; it can be expressed as: $\frac{L_{SSC}}{L_{sync}} = \frac{u_{sync}}{u_B}$, where the $u_{sync} = L_{sync}/(4\pi R^2 c\delta^4)$ is the energy density of the synchrotron photons, and $u_B = B^2/(8\pi)$ is magnetic field energy density. The beaming factor (δ) is then given from above equations:

$$\delta^2 = 1.6 \times 10^{12} \frac{L_{sync}}{cR^2} \left(\frac{L_{sync}}{L_{SSC}}\right) \frac{\nu_{SSC}^2}{\nu_{sync}^4} \frac{1}{(1+z)^2} \qquad (2)$$

An application of the synchrotron self-Compton (SSC) model to the overall spectral distribution and variability data of 18 blazars observed by *ASCA* implies that for the HBLs, the SSC model can indeed explain all available data quite well. Importantly, at least for Mkn 421, the parameters derived from it are in close agreement with those independently inferred from the spectral variability observed in the X–ray band by *ASCA* (see Sec. 4.1 below). The model implies relativistic Doppler factors δ in the range of 5 – 20, consistent with those derived from the VLBI data and from the limits inferred from γ–ray opacity to pair production, $\gamma\gamma \rightarrow e^+e^-$.

The situation in QHBs (and in some LBLs) is quite different. In the X–ray band observed by *ASCA* (0.7 – 10 keV), the QHBs have spectra that are hard, with $\alpha \sim 0.6$, and which are *not* located on the extrapolation of the synchrotron optical / UV spectra, but also apparently disjoint from the GeV HE component (cf. PKS 0528+134 in Fig. 1), suggesting that X–rays are likely to be due to a separate spectral component from GeV γ–rays. The application of the SSC model (thus assuming L_{HE} is solely due to the SSC component) implies that the values of δ derived from Eq. 2 are much in excess of values inferred from the γ–ray opacity arguments or the VLBI data (for details, see KTM98). This discrepancy can be eliminated if we adopt a scenario where the observed GeV γ–rays are produced by Comptonization of external photons (via the ERC process), while the GeV SSC flux is well below the ERC emission, and thus "hidden". In our analysis, we assumed that the the X–ray emission is produced via the SSC process, while the *observed* GeV γ–rays are produced by the ERC process.

In the context of this three-component scenario, we assume that the peak of the "hidden" SSC component can be still parameterized by L_{SSC} and ν_{SSC}. We assume that L_{SSC} and ν_{SSC} lie on or below the extrapolation of the $ASCA$ spectrum, but above the highest value of $\nu L(\nu)$ measured within the $ASCA$ band. Since the spectra of QHBs generally have $\alpha < 1$, the value of $\nu F(\nu)$ is the highest at the end of the $ASCA$ bandpass (at 10 keV $\simeq 2\times10^{18}$Hz) (see Fig. 3 in KTM98). Further constraints arise from Eq. 2: for an object with the observed L_{sync} and $\nu sync$, a selection of δ sets a unique relationship between L_{SSC} and ν_{SSC} such that $L_{SSC} = const \times (\nu_{SSC}/\delta)^2$. Since the VLBI data and γ–ray opacity arguments suggest that $5 < \delta < 20$ for most blazars (e.g. Vermeulen & Cohen 1994; Dondi & Ghisellini 1995), we adopt the values of 5 and 20 as lower and upper limits for δ. L_{SSC} and ν_{SSC} are then constrained to be inside the region defined from these conditions (for details, see KTM98). Once we obtain L_{SSC}, and ν_{SSC}, we can calculate the strength of the magnetic field B as follows:

$$B = 0.27 \left(\frac{R}{10^{-2}\mathrm{pc}}\right)^{-1} \left(\frac{\delta}{10}\right)^{-2} \sqrt{\left(\frac{L_{sync}}{10^{46}\mathrm{erg/s}}\right)\left(\frac{L_{sync}}{L_{SSC}}\right)} \quad \text{(Gauss)}, \quad (3)$$

and γ_{peak} is then calculated using Eq. 1.

Using the size of the emitting region estimated from the observed time variability via $R = c\Delta t\delta \;/\; (1+z)$, we infer B to be $0.05 \sim 1$ Gauss (using $\delta = 10$); B appears to be roughly similar for the two classes, but perhaps somewhat lower for HBLs than for QHBs. With these values of B, we estimate γ_{peak} to be lower, 10^3 – 10^4 for QHBs – where the LE component peaks at lower frequencies ($\nu_{LE} \sim 10^{13}$ – 10^{14} Hz) – and higher, $\sim 10^5$ – 10^6 for HBLs, where ν_{LE} is at 10^{16} – 10^{17} Hz. This is illustrated in Fig. 3, which shows the correlation between B and γ_{el}, where the HBLs preferentially occupy the right side of the diagram. This picture is consistent with the fact that the TeV emission has been observed only from the HBLs which turned out to have higher γ_{el}. This is because the energy conservation (or, equivalently, the Klein-Nishina limit) requires that Lorentz factors γ of $\sim 10^6$ are the minimum necessary to produce TeV photons. In the case of Mkn 421, the knowledge of γ_{peak} allows us to calculate the energy of the "seed" low energy photons $h\nu_{seed}$ via the standard

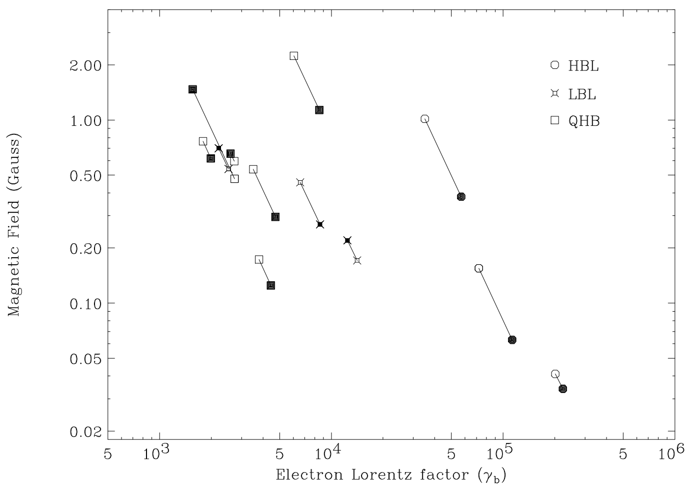

Fig. 3. Calculated magnetic field (B) versus Lorentz factor of electrons radiating at the peak of the $\nu F\nu$ spectrum (γ_{peak}). In the calculation, we use the beaming factor $\delta = 10$. The size R is estimated from the observed time variability (open symbols; see KTM98). We also plot values calculated with $R = 0.01$ pc (filled symbols).

Compton formula $h\nu_{SSC} \simeq \gamma_{peak}^2 \nu_{seed}$. For the TeV ($\sim 10^{25}$ Hz) radiation to be produced by Compton scattering, $h\nu_{seed}$ (as measured in the observer's frame; we assumed $\delta = 10$) must be around 0.1 - 1 eV. Interestingly, this means that the "seed" photons have *lower* frequency than ν_{LE}, where the energy density of the observed radiation spectrum peaks (around 0.1 – 1 keV).

As we argued above, for QHBs, where dense external radiation fields exist, the ERC emission most likely contributes more significantly than the SSC emission in the GeV γ–ray band (see, e. g., Sikora et al. 1997). This suggests that the difference of γ_{peak} between QHBs and HBLs can well be due to the larger total photon density in the jets of QHBs as compared with that of HBLs. In any case, these simple estimates can be refined only by introducing a detailed model of the jet, including its dynamics as well as its surroundings.

Recently, Ghisellini et al. (1998) performed detailed fitting based on the SSC and ERC model to multi-frequency spectra and obtained the same conclusion in that HBLs have higher γ_{el} than QHBs.

4 Multi-frequency Campaigns to Observe Mkn 421

Among the GeV-emitting blazars, the BL Lac object Mkn 421 is unique as the first – and so far, the brightest – member where the γ–ray emission extends up to the TeV energies at a level allowing detailed spectral and variability studies in the broadest range of wave bands. The simple continuum spectra of Mkn 421 from the radio to the UV and X–ray bands obtained previously imply that the emission from the LE component is due to the distribution of charged particles radiating via the synchrotron process (see, e.g., George, Warwick, & Bromage 1988). At TeV energies, flares with variability time scale as short as 15 minutes have been observed (Gaidos et al. 1996). In order to avoid absorption of γ–rays due to pair production, this fast variability requires a beaming factor $\delta > 9$.

4.1 1994 Observations

Study of variability patterns and the spectral evolution across different energy bands are the best (and perhaps the only) means to draw a general picture of non-thermal emission from blazars. The first multi-frequency observation from radio to TeV γ–rays, conducted in 1994, revealed a TeV flare detected by the *Whipple* Observatory (Kerrick et al. 1995), while the GeV γ–ray flux observed by *EGRET* was nearly constant. The 24 hr *ASCA* observation, started one day after the onset of the TeV flare, recorded a high level of 2 – 10 keV X–ray flux peaking at 3.7 $\times 10^{-10}$ ergs cm^{-2} s^{-1}, a 10-fold increase over the May 1993 value (Takahashi et al. 1996a). The flux level at other wavelengths such as radio and UV was roughly the same as that observed in the quiescent level (Macomb et al. 1995). The time history of Mkn 421 obtained from *ASCA* observation is shown in Fig. 4, together with the change of the hardness ratio. The GeV flux measured by *EGRET* (Macomb et al. 1995) and the flux above 500 GeV measured by *Whipple* telescope (Kerrick et al. 1995) are also shown in the figure. The doubling time scale is about a half day.

The 1994 *ASCA* observation revealed that the X–ray flux variability in Mkn 421 is correlated with the spectral changes such that the spectrum is generally harder when the source is brighter. In particular, the hard X–rays changed *first*, followed by changes to the soft X–ray flux, implying a "clockwise motion" in the flux vs photon index plane (cf. Fig. 7). Such behavior is typical at least for this particular BL Lac object and has been seen during earlier X–ray observations (cf. Tashiro 1992). High sensitivity measurements by *ASCA* allowed us for the first time to quantify the "soft lag." We measure the lag in several energy bands as compared to the 2 – 7.5 keV band using the cross correlation function of Edelson & Krolik (1988). The results are shown in Fig. 5: it appears that the hard X–ray variability leads that in softer X–rays by about 1 hour.

With the knowledge of δ – which we assume to be at least 5 – the discovery of the soft X–ray lag allows us to calculate the magnetic field from consideration of the synchrotron lifetime (cooling) of the relativistic electrons. The delay of the response of the soft X–ray flux implies that this may be due to the electron cooling effect, which is energy-dependent: the time τ_{sync} when an electron loses

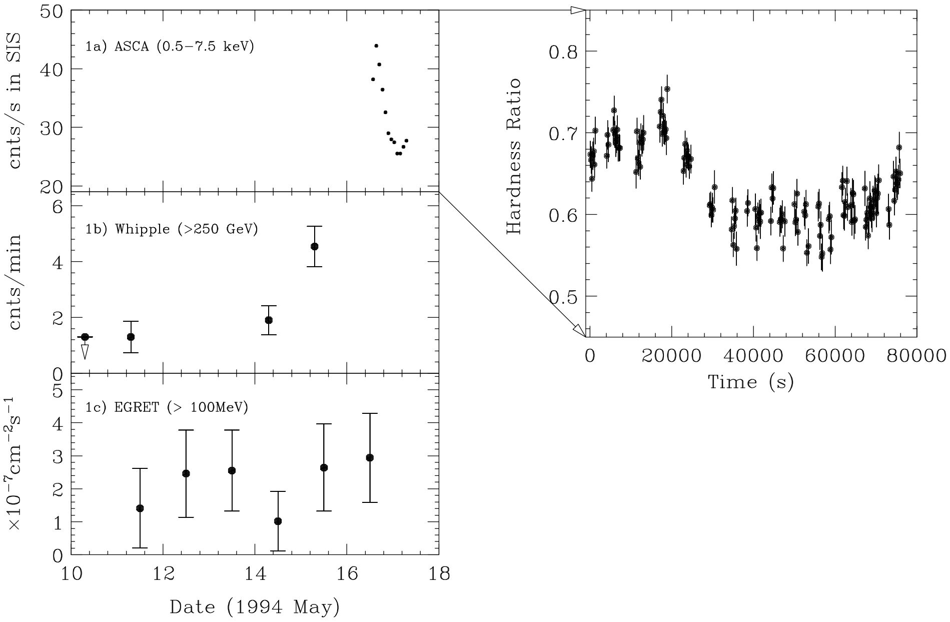

Fig. 4. Left panel: Time history of Mkn 421 emission obtained from *ASCA* (top), *Whipple* Telescope (middle), and *EGRET* (bottom) during the May 1994 campaign. The *ASCA* count rates are from the summed SIS0 and SIS1 data. Right panel: hardness ratio (1.5-7.5 keV)/(0.5-1.5 keV).

a half of its energy would roughly be (in the observer's frame) 5×10^8 B^{-2} γ_{el}^{-1} δ^{-1} s (cf. Rybicki & Lightman 1979). The peak observed frequency of the synchrotron emission ν_s by an electron with γ_{el} is given as $\nu_s \simeq 1.2 \times 10^6$ B γ_{el}^2 δ Hz for $z << 1$ (cf. Eq. 1). If E_{keV} is the observed energy in keV, τ_{sync} is then expressed as $\tau_{sync} \simeq 1.2 \times 10^3$ $B^{-3/2}$ $E_{keV}^{-1/2}$ $\delta^{-1/2}$ s. Since the lag is the difference of τ_{sync} at the different X–ray energies, we obtain $\tau_{sync} \sim 6000$ s at 1 keV (Fig. 5). If we take a beaming factor into account, τ_{sync} is given as $2 \times 10^3 B^{-3/2} E_{keV}^{-1/2} \delta^{-1/2}$, and B becomes $\sim$ 0.2 Gauss for $\delta \sim 5$. This, in turn, yields $\gamma_{\rm el} \sim 5 \times 10^5 (E/(1 \text{ keV})^{1/2})$, consistent with the value obtained by multi-frequency analysis described above (also see Tavecchio, Maraschi, & Ghisellini 1998)

Mastichiadis & Kirk (1997) demonstrate that the flares of Mkn 421 are due to short-lived increase in the upper cutoff-energy of freshly injected electrons, while keeping the electron energy distribution and the magnetic field constant. Theoretical interpretation of the clockwise motion has been discussed in Kirk et al. (1998) and Dermer (1998), in terms of the balance between time scales of electron cooling and expansion of the emitting region.

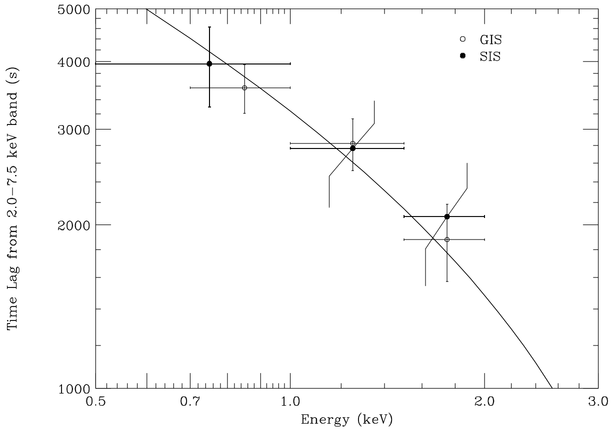

Fig. 5. Time lag of photons from Mkn 421 of various X–ray energies against the 2 - 7.5 keV band photons, calculated using the discrete correlation function (DCF) with data obtained in 1994 observation, The solid line corresponds to a fit with $\tau_{sync}(E) - \tau_{sync}(5\mathrm{keV}) = 1.2 \times 10^3\ B^{-3/2}\ \delta^{-1/2}\ (E_{keV}^{-1/2} - (5)^{-1/2})$, which, for $\delta = 5$, yields $B \simeq 0.2$ Gauss, and $\tau_{sync}(1\mathrm{keV}) \simeq 6000$ sec (Takahashi et al. 1996a).

4.2 1995 Observations

In 1995, the X–ray observations started almost simultaneously with the rise of the TeV flare (Buckley et al. 1996). In the campaign, short observations of 8 – 10 ks with *ASCA* were spaced between 1 to 3 days apart, such that it covered the TeV observations (Takahashi et al. 1996b). Main aim was to monitor long term stability, rather than the short term behavior we obtained in 1994. The normalized light curve obtained from the summed SIS0 and SIS1 data is shown in Fig. 6, together with TeV data (Buckley et al. 1996), EUV data (Kartje et al. 1996) and optical data (Wagner 1996). The variations shown on Fig. 6 are fairly similar in shape in all four energy bands. Although the peak-to peak amplitude is only 10 % in the optical band, Mkn 421 shows variations which appear to be correlated over an energy range of 13 decades of frequency, the widest energy range over which such simultaneous changes have been observed so far. The X–ray emission does track (including the relative amplitude) the general rise and decline seen in the TeV γ–rays. It is clear, however, that the variability of the X–ray flux has two components, one on a $\sim$ one-day time scale as detected in the X–ray flare in 1994 (Takahashi et al. 1996a) and the other on a $\sim$ one-week time scale. The best continuous coverage of the flare was obtained by *EUVE* which resolved the smooth rise and full of the flux, with variability of as much as a factor of $\sim$1.5 over a span of $\sim$ 2 days (Kartje et al. 1997).

The X–ray flux was at a similar level to that obtained in the X–ray/TeV flare detected in 1994. The X–ray flux changed from 2.3 to 0.4 $\times 10^{-10}$ erg cm^{-2} s^{-1}. A correlation between flux and the photon index as fitted to a simple power law with free absorption is shown in Fig. 7 (which also shows the 1994 data).

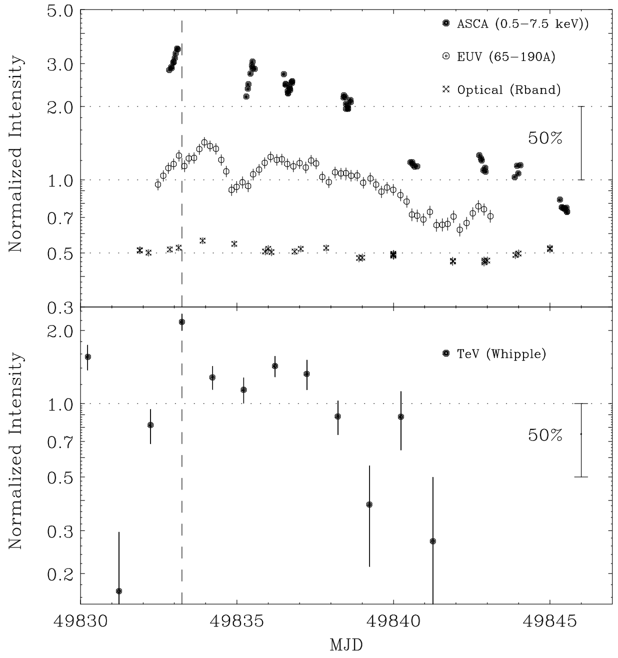

Fig. 6. Upper panel shows Normalized X–ray (Takahashi et al. 1996b), extreme-UV (Kartje et al. 1997), and optical (Wagner 1996) light curves for Mkn 421 taken during the 1995 April-May multiwavelength campaign. Lower panel shows the normalized light curve of TeV γ–rays (Buckley et al. 1996).

There is a general tendency, both in one-day observation (1994) and two-weeks observation (1995), that the spectrum becomes soft when the source is faint. In both 1994 and 1995 observations, the X–ray spectra steepen towards higher energies and a single power-law function and the absorbing column N_H fixed at the Galactic value does not fit any of the spectra well. Instead, the peak frequency appears to shift from $\sim$ 1.4 keV to $\sim$ 0.7 keV when the flux decreases (cf. Fig. 8). Again, there was a spectral variability within each "sub-segment", where the harder X–rays varied faster than the soft X–rays. However, we could not obtain the time-lag between two energy bands due to short observation time compared with the campaign in 1994. Although the observations were not truly simultaneous, the amplitudes of the X–ray and TeV γ–ray flux variability were nearly the same during the decay portion of the observations.

4.3 1998 Campaign

Judging by the results of previous campaigns which included TeV observations, correlations of inter-band variability of Mkn 421 have proven to provide our best opportunity to understand the high energy emission from blazar jets. In particular, the rapid intra-day variability seen in both X–ray and TeV energy bands gives us clues to study the physics of blazar jets. However, the sparse

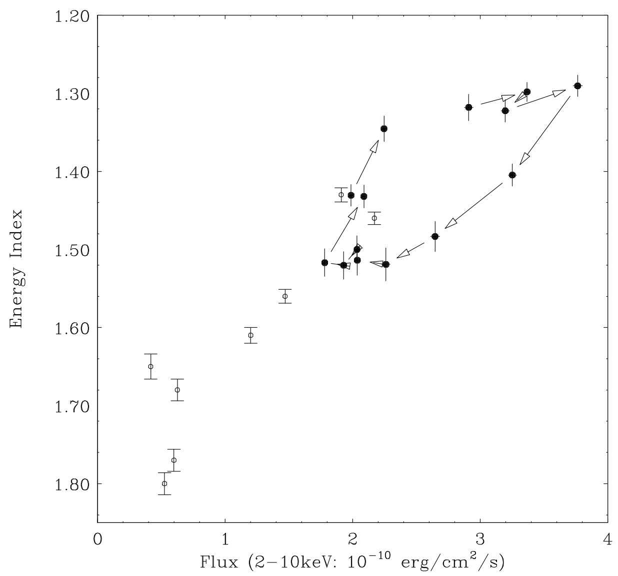

Fig. 7. The evolution of the X–ray spectrum of Mkn 421 as a function of the X–ray flux. The model is a power law with free absorption for data obtained in 1994 (filled circles) and 1995 (open circles).

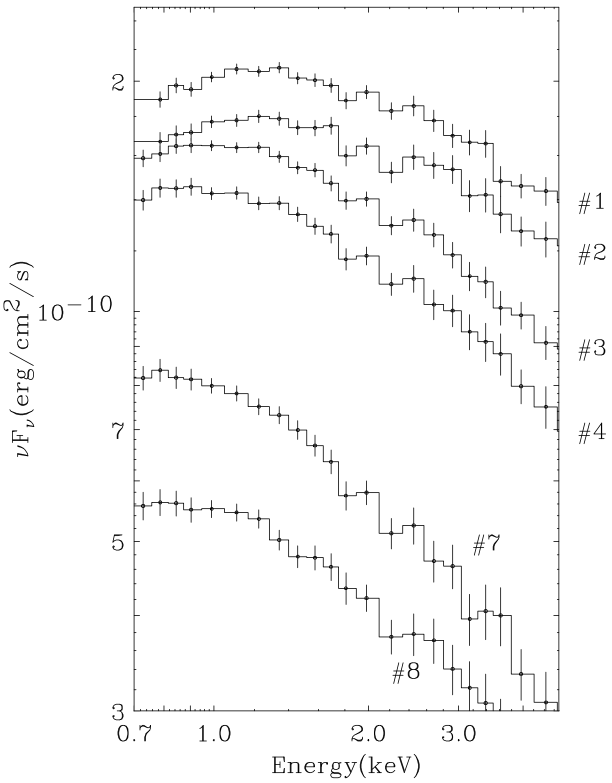

Fig. 8. The evolution of the X–ray spectrum in $\nu F \nu$ space for data obtained in 1995. The shift of the peak frequency observed in the declining phase during the 2 weeks campaign is clearly seen.

sampling of the previous campaigns has prevented us from obtaining definitive conclusions. Inter-band correlations can only be confirmed unambiguously if the observations are truly simultaneous and if they extend for a period longer than several times the characteristic time scale.

With this in mind, we proposed an unprecedented seven-day continuous observations with *ASCA* (PI Takahashi), coordinated with EUVE (10 days continuous; PI Takahashi), RXTE (low background orbits only; PI Madejski) and SAX (two 60 ks observations, one is on April 21-22 and the other is April 23-24; PI Chiappetti). At the same time, TeV detectors (CAT, HEGRA, and Whipple), optical telescopes (coordinated by Mattox), and 22 GHz radio antennae (by Terasranta) attempted to observe the source every night. Here we present the preliminary results of the campaign; the SAX results are presented elsewhere in these proceedings (cf. article by Maraschi et al.).

ASCA observation was performed during 1998 April 23.97 – 30.8 UT, yielding a net exposure of $\sim$ 280 ks. The time history of this observation obtained from the SIS detectors is shown in Fig. 9b, together with that in the TeV (Fig. 9a), although the TeV observations are much sparser than those by *ASCA* . The 2 - 10 keV flux in the beginning of the observation was 1.2×10^{-10} erg cm^{-2} s^{-1} and increased up to 5.0×10^{-10} erg cm^{-2} s^{-1} at the maximum. More than 10 flares are clearly seen superimposed on the general increasing trend. The doubling time scale of each flare is about 0.5 days. Continuous light curve of 7 days implies that the source actually flares daily, and perhaps more often. Even though Mkn 421 is a bright X–ray emitter, this behavior is hard to study in any detail with the All Sky Monitor on board RXTE: our observation demonstrated that a large and sensitive detector is indispensable for the study of variability in blazars.

The X–ray light curve contains multiple flares with time scale of 0.5 – 1 day, superimposed on the general trend of gradually increasing flux. This is very similar to that seen in optical light curves of QHBs, where the high energy component peaks at GeV γ–ray energy band (Wagner et al. 1996). This is consistent with the idea that the largest amplitude of the rapid variability is caused by the highest energy end of the electron distribution. The synchrotron emission due to these electrons corresponds to eV range for QHBs and to keV range for HBLs such as Mkn 421. A good scenario would that either the "blob" of plasma passed through the spatial region where shock are formed, or there is some sort of standing shock in the jet, which is much larger than a shock. Note that the particles can also escape upon crossing the source.

ASCA data clearly reveal spectral variability, seen as the time variation of the hardness ratio in Fig. 9c. The 2 – 7 keV energy index ranges from 1.4 to 1.8. The comparison of the data from *ASCA* , EUVE and RXTE indicates that the variability amplitudes in the LE (synchrotron) component are larger at higher photon energies. TeV light curve does show the same general trend, if the cross-calibration among the three participating TeV telescopes are accurate.

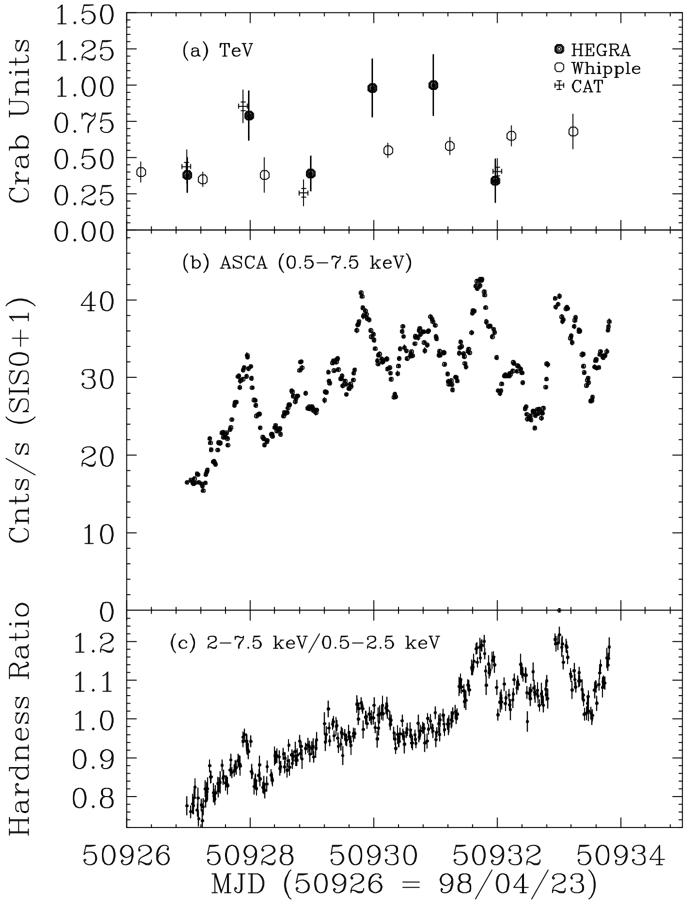

Fig. 9. 1998 campaign for Mkn 421: (a) TeV light curves obtained by Whipple (Weekes et al. 1999, in preparation), HEGRA (Aharonian et al. 1999, in preparation) and CAT (Degrange et al. 1999, in preparation) Cherenkov telescopes. (b) *ASCA* light curve (summed SIS0 and SIS1 data). (c) Evolution of the hardness ratio measured in the *ASCA* X–ray data (2.0 – 7.5 keV)/(0.5 – 2.0 keV).

Fig. 10 shows the correlation between TeV flux by the Whipple telescope and X–ray flux by *ASCA* . It should be noted that the data were obtained from truly simultaneous observations. In addition to the correlation between 7-day *ASCA* observation, one complete flare was recorded by *SAX*and the Whipple telescope in the observation carried out as a part of the 1998 campaign, but immediately preceding the *ASCA* observation (Maraschi et al., these proceedings). Detailed analysis of the evolution of the multi-frequency spectrum and shape of flares obtained from the campaign will be presented elsewhere (Takahashi et al. 1999, in preparation).

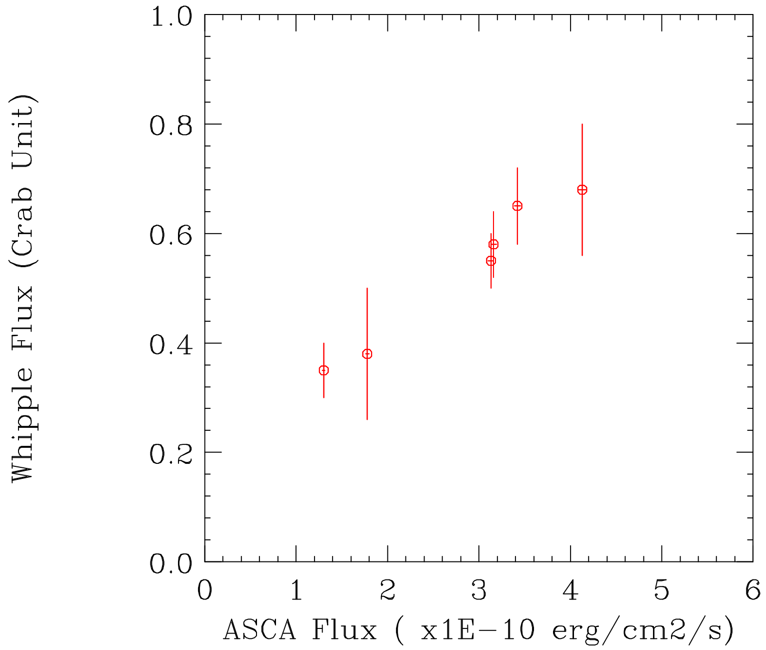

Fig. 10. Correlation between 2 – 10 keV flux by *ASCA* and the TeV γ–ray flux obtained by the Whipple telescope during 1998 campaign. Observations are truly simultaneous.

5 Summary and Conclusions

The *ASCA* data – and, specifically, the spectral variability detected with its sensitive instruments, in the context of the multi-frequency analysis – allow an investigation of the details of the emission in blazar jets, and in particular, an estimate of the physical parameters, such as B and γ_{el}. An application of the synchrotron self-Compton (SSC) model to the overall spectral distribution and variability data for HBL-type blazars observed by *ASCA* implies that the SSC model can explain all available data quite well. In particular, the values physical parameters of the radiating plasma inferred from the energetics requirement to produce the TeV γ–rays agree well with those inferred from the spectral variability observed in X–rays. This model implies relativistic Doppler factors δ in the range of 5 - 20, consistent with the those derived from the VLBI data and from the limits inferred from γ–ray opacity to pair production, $\gamma\gamma \rightarrow e^+e^-$. This is in contrast to QHBs, where the simple SSC models fail. Instead, a three-component model, with the low energy peak due to synchrotron radiation, the X–ray emission produced by the SSC process, and MeV / GeV γ–ray emission due to Comptonization of external radiation photons, describes the observed data well.

Previous multi-frequency campaigns of Mkn 421 with *ASCA* and the Whipple TeV telescope showed a very important connection between the X–ray and the TeV energy bands. These observations are very suggestive but not conclusive because of sparse sampling during flares which occur on a time scale of $\sim 1/2-$ 1 day to one week. The great success of the big campaign conducted in 1998 is in providing valuable information about blazar jets via the measurement of spectral evolution of the emitted radiation, but, importantly, it also motivates the further development of time dependent models for the structure of blazar jets, and acceleration of particles in these jets.

Acknowledgements

The collaborators of the Mkn 421 campaign in 1998 include T. Takahashi, F. Aharonian, M. Catanese, L. Chiappetti, P. Coppi, B. Degrange, R. Edelson, H.Kubo, J. Kataoka, G. Madejski, F. Makino, H. Marshall, L. Maraschi, J. Mattox, E. Pian, F. Takahara, M. Tashiro, H. Terasranta, C. M. Urry, S. Wagner, and T. Weekes. We thank the CAT, HEGRA, and Whipple teams for providing with their data before publication; and J. Kataoka and K. Yamaoka for the help of analysis of *ASCA* data.

References

[1] Blandford, R. D., & Konigl, A. 1979, ApJ, 232, 34
[2] Blandford, R. D., & Levinson, A. 1995, ApJ, 441, 79
[3] Brinkmann, W., et al. 1994, A&A, 288, 433
[4] Buckley, J. H., et al. 1996, ApJ, 472, L9
[5] Catanese, M. A., et al. 1998, ApJ, 501, 616
[6] Catanese, M. A., et al. 1997, ApJ, 487, L143
[7] Chadwick, P. M., et al. 1998, ApJ, in press (astro-ph/9810263)
[8] Comastri, A., et al. 1997, ApJ, 480, 534
[9] Dermer, C. D., Schlickeiser, R., & Mastichiadis, A. 1992, A & A, 256, L27
[10] Dermer, C. D. 1998, ApJ, 501, L157
[11] Dondi, L., & Ghisellini, G. 1996, MNRAS, 273, 583
[12] Edelson, R. A. & Krolik, J. H. 1988, ApJ, 333, 646
[13] Gaidos, J. A., et al. 1996, Nature, 383, 319
[14] George, I. M., Warwick, R. S., & Bromage, G. E. 1988, MNRAS, 235, 787
[15] Ghisellini, G. & Maraschi, L. 1989, ApJ, 340, 181
[16] Ghisellini, G., et al. 1998, MNRAS, 301, 451
[17] Inoue, S. & Takahara, F. 1996, ApJ, 463, 555
[18] Kartje, J., et al. 1997, ApJ, 474, 630
[19] Kataoka, J., et al. 1999, ApJ, in press
[20] Kerrick, A. D., et al. 1995, ApJ, 438, L59
[21] Kirk, A. D., et al. 1998, A&A, 333, 452

[22] Konigl, A. 1981, ApJ, 243, 700
[23] Kubo, H., 1997, Ph.D.Thesis, University of Tokyo
[24] Kubo, H., Takahashi. T., Madejski, G. M., Tashiro, M., Makino, F., Inoue, S., & Takahara, F. (KTM98) 1998, ApJ, 504, 693
[25] Macomb, D., et al. 1995, ApJ, 449, L99 (erratum 459, L111 [1996])
[26] Mastichiadis, A., & Kirk, J. G. 1997, A&A, 320, 19
[27] Mukherjee, R. et al. 1997, ApJ, 490, 116
[28] Mattox, J. R., et al. 1993, ApJ, 410, 609
[29] Padovani, P., Giommi, P., & Fiore, F. 1997, MNRAS, 284, 569
[30] Pian, M., et al. 1998, ApJ, 490, L17
[31] Punch, M., et al. 1992, Nature, 358, 477
[32] Quinn, J., et al. 1996, ApJ, 456, L83
[33] Rees, M. 1967, MNRAS, 137, 429
[34] Rybicki, G. B. & Lightman, A. P. 1979, Radiative Processes in Astrophysics (New York: Wiley Interscience)
[35] Sambruna, R. M., Maraschi, L., & Urry, C. M. 1996, 463, 444
[36] Sambruna, R. M. 1997, ApJ, 487, 536
[37] Sikora, M., Madejski, G., Moderski, R., & Poutanen, J. 1997, ApJ, 484, 108
[38] Sikora, M., Begelman, M. C., & Rees, M. J. 1994, ApJ, 421, 153
[39] Takahashi, T., et al. 1996a, ApJ, 470, L89
[40] Takahashi, T., et al. 1996b, Mem. Soc. Astron. Ital., 67, 533
[41] Takahashi, T., Kubo, H., Madejski, G. M., Tashiro, M., & Makino, F. 1997, in *Proceedings of the Fourth Compton Symposium*, C. D. Dermer, M. S. Strickman, & J. D. Kurfess, eds., AIP Conference Proceedings, 410, 1467
[42] Tashiro, M. 1992, Ph.D. Thesis, University of Tokyo
[43] Tavecchio, F., Maraschi, L., & Ghisellini, G. 1998, ApJ, 509, 608
[44] Urry, C. M. et al., 1997, ApJ, 486, 799
[45] Vermeulen, R. C., & Cohen, M. H. 1994, ApJ, 430, 467
[46] von Montigny, C., et al. 1995, ApJ, 440, 525
[47] Wagner, S. J. 1996, A&A Suppl 120, C495
[48] Wagner, S. J., et al. 1996, AJ, 111, 2187